Thermal, Hydrolytic, Anticorrosive, and Tribological Properties of Alkyd-Silicone Hyperbranched Resins with High Solid Content

Edwin A. Murillo,[1,2,3] Betty L. López,[2,3] Witold Brostow[1]

[1]*Laboratory of Advanced Polymers & Optimized Materials (LAPOM), Department of Materials Science and Engineering and Center for Advanced Research and Technology (CART), University of North Texas, 3940 North Elm Street, Denton, TX 76207*
[2]*Grupo Ciencia de los Materiales, Instituto de Química, Universidad de Antioquia, Calle 62, 52 59 Medellín, Antioquia, Colombia*
[3]*Departamento de Ingeniería Metalúrgica y de Materiales, Universidad de Antioquia, Calle 67 Número 53-108 Medellín, Antioquia, Colombia*

Received 2 August 2010; accepted 4 April 2011
DOI 10.1002/app.34611
Published online 22 November 2011 in Wiley Online Library (wileyonlinelibrary.com).

ABSTRACT: Novel alkyd hyperbranched resins (AHBRs) modified with a Z-6018 silicone (a polysiloxane intermediate) and with high solid content were synthesized by etherification reaction using an acid catalyst. Different molar ratios of AHBR to silicone were used. Structural, thermal, hydrolytic, anticorrosive, and tribological properties were studied using infrared (IR) analysis, nuclear magnetic resonance (NMR), vapor pressure osmometry (VPO), thermogravimetric analysis (TGA), acid value, electrochemical impedance spectroscopy (EIS), and pin-on-disk friction. IR and NMR provide evidence of grafting of the silicone on AHBR; the efficiency of grafting was quantified by TGA. Thermal stability was studied also by acid value analysis. Grafting increases the number average molecular mass, enhances thermal stability, and improves significantly hydrolytic stability. Corrosion resistance on steel is improved by two orders of magnitude, hence our modified materials can be used as highly effective anticorrosion coatings. Grafting lowers dynamic friction dramatically, more so at higher concentrations of silicone. © 2011 Wiley Periodicals, Inc. J Appl Polym Sci 124: 3591–3599, 2012

Key words: silicone resins; anticorrosion coatings; etherification; thermal stability; friction lowering

INTRODUCTION

Polymeric coatings have a variety of applications.[1–5] However, the coatings industry is undergoing a transformation toward reduction of volatile organic compounds (VOCs). Some routes for reducing the VOCs emitted by coatings are well known; examples include powder coatings, waterborne coatings and high-solids coatings. Due to low baking temperature and simple equipment required, the preferred route to reduce the VOCs is making high-solids coatings.[6]

Hyperbranched polymers (HBPs) can be synthesized by: one step polymerization;[7] step-by-step[8]; or a combination of one step and step-by-step methods.[9]

These polymers have large numbers of surface functionalities, no entanglements in the structure, low melt or low solution viscosity—this in contrast to linear polymers.[10] HBPs have end-groups in the periphery—this has important effects on their physical and chemical properties. The solubility depends to a large extent on the structure of the end-groups.[11] Properties of HBPs can be tailored by modifying end-groups for specific applications such as cross-linkers,[12] high solid coatings,[13] and thermosets.[14] Since hydroxylated hyperbranched polyesters have high numbers of OH groups in the periphery (terminal units), they can be modified with acids, amines, anhydrides, hydroxylated silicone, or isocyanates for obtaining a variety of polymers. Alkyd hyperbranched resins (AHBRs) are hydroxylated hyperbranched polyesters modified with fatty acids (Fig. 1). Filled circles in the Figure represent branching points. Conventional alkyd resins have linear structures; these resins due to their high hydrodynamic volumes have high viscosity in comparison to hyperbranched alkyd resins of the same molar mass.[15] This is due to the latter's highly branched, compact and globular nonentangled structures.[14,15] AHBRs have good gloss, flexibility, and good adhesion[16] but low hardness.[13]

For obtaining an AHBR, some terminal OH groups in the periphery of HBPs are modified with fatty acids by esterification reaction. Terminal OH groups that have not reacted (residual OH groups) may be used for hybridizing the AHBR with others material, so the AHBR can be hybridized to improve its properties. Coatings for some applications such as protective films, decorative paints, water repellants, antifoaming

Correspondence to: W. Brostow (wbrostow@yahoo.com).

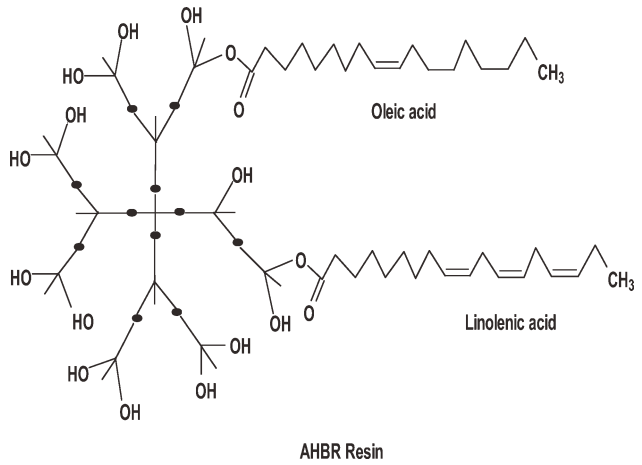

Figure 1 Chemical structures of alkyd hyperbranched resins.

agents need to have good resistance to water, to corrosion, low friction, thermal stability, and furthermore gloss and high hardness.[16–18]

Silicone resins due to Si—O bonds and partially ionic character have good thermal, oxidative, and ultraviolet degradation resistance.[19] These properties can be incorporated into conventional alkyd resins through chemical reactions between the silicone with residual OH groups in the conventional alkyd resin. Water that is liberated has to be removed to achieve completion of the reaction.[19–21]

Silicone intermediates have been used to modify organic resins to improve their properties. Thus, alkyd resins were mixed with silica and isocyanates to create dental obturation materials.[22] A conventional alkyd resin (with linear structure) based on soybean oil was modified with a silicone/acrylic copolymer to achieve improvement of mechanical properties.[23]

Mechanical properties of polymer-based materials are being studied extensively.[24] Studies of tribological properties of polymers exist[25–28] but are much less frequent for resins. Such studies of hyperbranched alkyd resins have not been reported—despite the importance of wear for industry and economics. In this work, an AHBR which contains OH groups and fatty acid chains in the periphery (Fig. 1) has been modified with varying amounts of Z-6018 silicone by an etherification reaction between OH groups of the alkyd resin with OH groups of a hydroxylated silicone. Effects of the silicone content on the structural, thermal, hydrolytic, anticorrosive and tribological properties of alkyd-silicone hyperbranched resins (ASiHBRs) have been studied.

EXPERIMENTAL

Materials

Hydroxyl-terminated silicone intermediates (Z-6018 silicone) with the glass transition temperature T_g = 77.3°C, viscosity-average molecular weight $M_v = 1.6 \times 10^2$ and Si content = 22.5%[29] was obtained from Dow Corning. Xylene, tetrahydrofurane (THF), potassium hydroxide (KOH), and *p*-toluenesulfonic acid (PTSA) were purchased from Sigma Aldrich and they were used as received. Cobalt, calcium, and zirconium octoate were supplied from Colorquímica and also used as received.

Synthesis of ASiHBRs

Grafted resins, to be called ASiHBRs, were synthesized in our group; details of the synthesis procedure and properties were reported in earlier publications.[30,31] Our AHBR was mixed with an appropriate amount of Z-6018 silicone in the presence of an acid catalyst (PTSA). The system was heated (80–150°C) under constant mixing and nitrogen atmosphere. Previously, the optimum time range for the reaction without gelation taking place was determined (0.5–2 h); this time was the same in all cases. Finally, xylene was added to the reactor, resulting in formation of ASiHBRs with the solid content of ≈70 wt %. Figure 2 provides a schematic

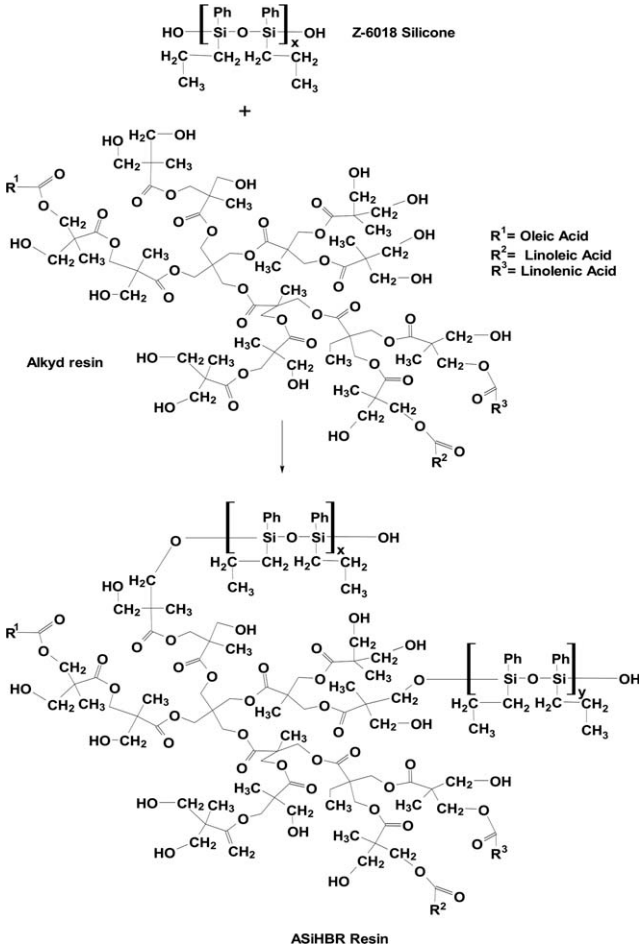

Figure 2 Schematic representation of the synthesis.

TABLE I
Molar Ratios of Z-6018 Silicone Compound to AHBR and Initial Percentages of Si in the Synthesis of ASiHBRs

Resins	Z-6018/AHBR Ratio	Si Initial Percentage
ASiHBR1	0.34	2.04
ASiHBR2	0.62	3.75
ASiHBR3	0.86	5.19
ASiHBR4	1.06	7.23

representation of the synthesis. The molar ratios of Z-6018 silicone to AHBR and initial percentages of Si in the resins are reported in Table I; these values were calculated from the proportion of Z-6018 silicone employed in the synthesis of each ASiHBR.

Methods

Structural analysis

Before the analysis, samples were submitted to Soxhlet extraction for 24 h with hexane as solvent so as to eliminate Z-6018 silicone residues.[32] For infrared (IR) analysis we have used a Perkin–Elmer Spectrum One spectrometer between 4000 and 450 cm^{-1}, performing eight scans at 4 cm^{-1} resolution. The nuclear magnetic resonance (NMR) analyses were carried out in a Brukker AC 300 MHz spectrometer. The ^{1}H-NMR spectrum was obtained using deuterated chloroform as solvent.

The vapor pressure osmometry analysis (VPO) for determining the number average molar mass M_n was carried out in a Knauer vapor pressure osmometer using THF as solvent in the concentration range from 1.14 to 9.04 g kg^{-1} at 45°C. Benzil(2-diphenyl-1,2-ethanedione) was used for calibration. Each experiment was repeated five times and the data reported are averages.

Thermogravimetric analysis (TGA)

Samples were first purified as reported before.[32] Thermal degradation of ASiHBRs and progress of the reaction reflected in Si content were determined by TGA using a TA instrument model Q500 in nitrogen and air atmosphere at the heating rate of 10°C min^{-1}. Amounts of Si in each ASiHBR were obtained from stoichiometric calculations on the basis of the weight of the initial sample and of the SiO_2 residue after a TGA run.

Hydrolytic stability

Each ASiHBR was mixed with water until an emulsion was formed and then stored at 50°C for 28 days. To determine the acid value (AV), the resins were taken out of the oven and kept at room temperature. Afterwards a 10 mL mixture of solvent xylene + isopropyl alcohol (neutralized) was added to dilute the sample and titrated with 0.46*M* KOH standard solution using phenolphthalein as an indicator.

Anticorrosive properties

To analyze film properties, the ASiHBRs were mixed with equal volumes of solutions of cobalt octoate (0–4 wt %), calcium octoate (0–4 wt %) and zirconium octoate (also 0–4 wt %). By using a film applicator, the resins films were applied on steel surfaces and dried at 25°C. The anticorrosive properties of the films were studied by electrochemical impedance spectroscopy (EIS). EIS measurements were performed using a potentiostat/galvanostat (Autolab Ecochemie). The exposed area of the working electrode was 1 cm^2, platinum was used as the counter electrode and an Ag/AgCl electrode was used as the reference. The positions of all electrodes were fixed within the cell configuration.

Frequency scans were carried out by applying a 10 mV amplitude sinusoidal wave. The frequency range covered was from 100 kHz to 5 mHz and the electrolyte an aqueous sodium chloride solution (3.5 wt %).

Tribological properties

Resin films were obtained in the same manner as was previously described for EIS analysis. Dynamic friction was determined using a pin-on-disk Nanovea machine with the following parameters: disk speed = 100 rpm; pin diameter = 4.0 mm; 2000 revolutions at the applied load = 2.0*N*. The thickness of films was the same in all cases (50 μm), determined with an Elcometer apparatus.

STRUCTURAL ANALYSIS

To verify grafting of Z-6018 silicone compound onto AHBR, we have performed IR analysis, NMR, and VPO. For brevity, we report here IR and NMR results for ASiHBR1 which contains the lowest amount of initial Si.

Infrared analysis

We present IR spectra of the Z-6018 silicone compound [Fig. 3(a)], AHBR [Fig. 3(b)] and ASiHBR1 [Fig. 3(c)]. In Figure 3(a), we see several signals: that at 3401 cm^{-1} corresponds to Si—OH, at 3030 cm^{-1} to aromatic C—H stretching, around 2955 cm^{-1} to aliphatic C—H stretching, the overtone between 1667 and 2000 cm^{-1} to monosubstituted aromatic rings, while signals at 1595, 1492, and 1134 cm^{-1}

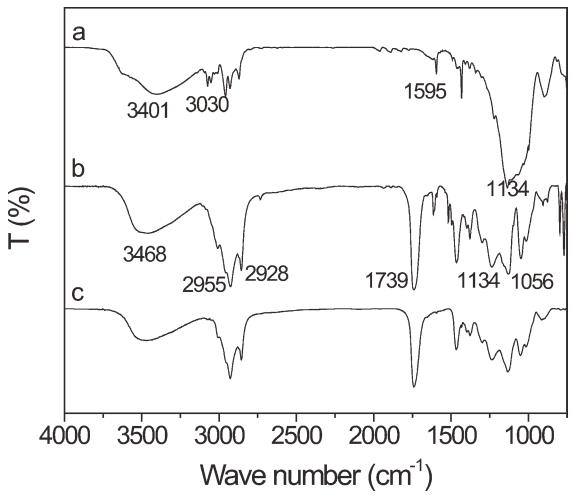

Figure 3 Infrared spectra.

correspond respectively, to C=C ring stretching, Si—O—C stretching and Si—O—Si bond vibrations. Around 800 cm^{-1} we see a band corresponding to the Si—O—Si symmetric stretch.

In Figure 3(b) we see the signal at 3468 cm^{-1} due to OH group, the signal at 3002 cm^{-1} corresponds to CH=CH stretching of fatty acids, the signal at 1741 cm^{-1} is assigned to C=O bonds of ester groups. The signals that appear around of 1200 cm^{-1} are assigned to ester (—COOR) and ether (C—O—C) groups. Around 800 cm^{-1} there is a signal due to bending of C=C bonds of the AHBR. The signal of ether groups in the resin spectrum corresponds to the etherification reaction that took place during the synthesis of a hyperbranched polyol polyester employed in preparation of AHBR.

Figure 3(c) shows a signal at 3468 cm^{-1} of lower intensity with respect to this signal in the original resin [Fig. 3(b)]. The signal assigned to aromatic rings reflects successful formation of ASiHBR1. The signals at 1134 and 1056 cm^{-1} are due to bond vibrations Si—O—C, C—O—C and Si—O—Si. The signal that appears around 800 cm^{-1} possibly overlaps with a signal that appears in the same region for Z-6018 silicone [Fig. 3(a)] and for AHBR [Fig. 3(b)]. Reduction of intensity of peaks representing C—OH and Si—OH groups are indications of the etherification reaction between OH groups of the AHBR and the silicone compound.

NMR RESULTS

Figure 4 shows the ^1H NMR spectrum of the ASiHBR1 resin. The signals that appear between 7.0 and 7.35 ppm are assigned to the chloroform (solvent) and aromatic protons joined to Si atoms [Fig. 4(a)]; these signals are better seen in a magnified spectrum of this region [Fig. 4(b)].

The protons of the aromatic rings near to Si atoms appear in the range 7.25–7.35 ppm. Between 5 and 6 ppm, we see a signal of CH=CH protons of fatty acids of AHBR; the signal at 4.23 ppm is assigned to the methylene groups in vicinity of the reacted hydroxyl groups (—CH_2OR); the signals between 3.4 and 3.6 ppm correspond to the methylene groups joined to OH groups (—CH_2OH) or Si—O (SiOCH_2R). The signal between 0.5 and 2.8 ppm is assigned to aliphatic protons (CH_2, CH and CH_3).

VAPOR PRESSURE OSMOMETRY

This method relies on a basic fact: vapor pressure of a solution is lower than that of the pure solvent at the same temperature and pressure. The decrease of vapor pressure is directly proportional to the molar concentration of the dissolved polymer—this can be used to obtain number average molar mass M_n.[33] The determination of M_n of HBPs and dendrimers by VPO is independent of the structure of the samples. This in contrast to gel permeation chromatography (GPC) which depends on hydrodynamic volume of the sample.

That volume for linear polymers can be higher than for hyperbranched and dendrimers polymers.

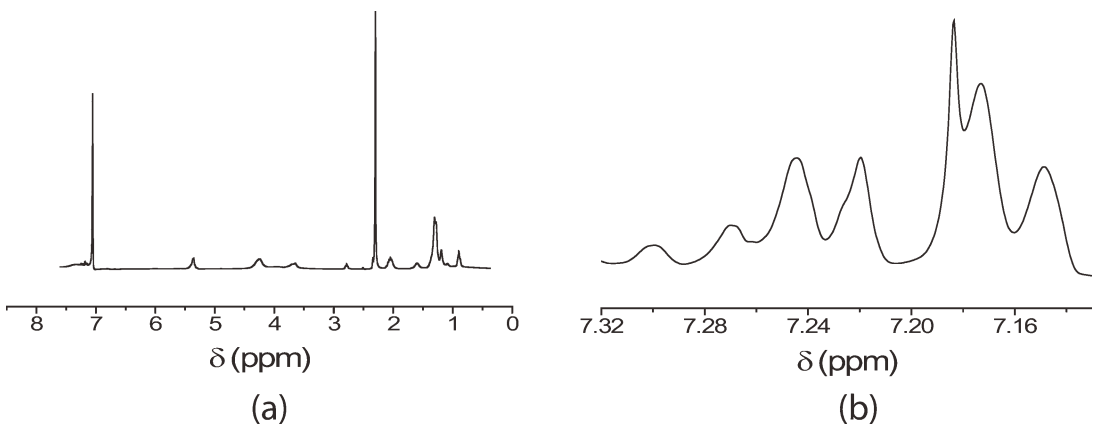

Figure 4 ^1H NMR spectrum of the ASiHBR1 resin.

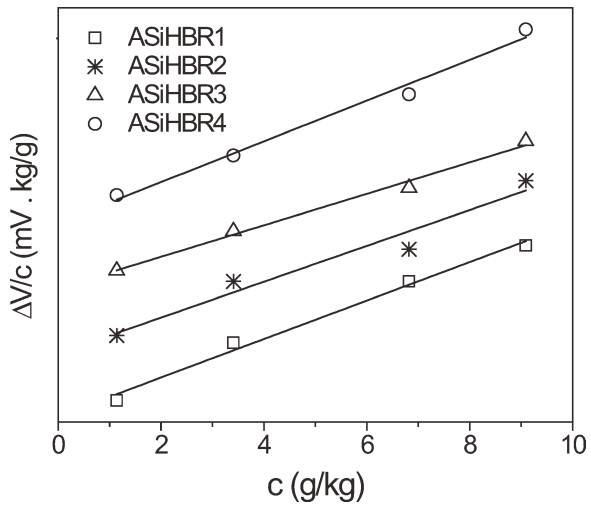

Figure 5 $\Delta V/c$ as a function of concentration.

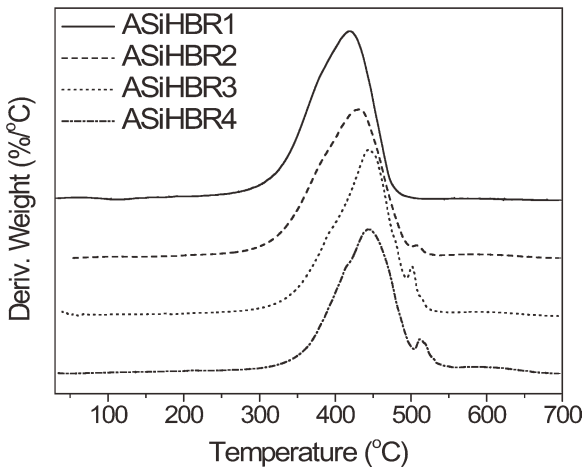

Figure 6 Derivative weight as a function of temperature.

Here lies a possible cause for an error since GPC calibration plots typically pertain to linear standards (polystyrene, polyacrylates). M_n values have been calculated as

$$\Delta V/c = K_c/M_n + K_c A_2 \rho c \quad (1)$$

Here ΔV, c, K_c, A_2, and ρ are, respectively, the potential change measured by the change in resistance of the thermistor, the concentration in the solution in g kg^{-1}, a calibration constant, the second virial coefficient and the mass density of the solvent. The value of K_c was determined from the intercept of benzil calibration curve and is = 167 mV kg mol^{-1}.[31] Using eq. (1) and Figure 5, we have calculated the M_n values of the ASiHBRs. Table II shows M_n, intercept and correlation factors values for our ASiHBRs. The M_n values increase along with the amount of the silicone compound employed in the synthesis. They are higher than $M_n = 5.95 \times 10^3$ g mol^{-1} obtained for the starting AHBR.[31] The correlation factors are satisfactory. Clearly modification with silicone was successful.

THERMOGRAVIMETRY RESULTS

Figure 6 shows plots of the derivate weight versus temperature T of our ASiHBRs in nitrogen atmosphere. Several degradation regions are seen. The first large peak T_{d1} which begins around 350°C represents decomposition of AHBR. The degradation T_{d2} around 500°C reflects partial degradation of the silicone in the resins.[31] This degradation possibly is due to the aliphatic part of the silicone since the aromatic part is known to be more thermally stable.

The T_{d1} loss peaks move to higher temperatures with increasing silicone content. The T_{d2} peak is the largest for ASiHBR4 and hardly visible for ASiHBR1, a consequence of the largest and smallest concentration of Si, respectively. Figure 7 shows thermograms obtained in air atmosphere. Since in nitrogen atmosphere the combustion is incomplete, we had residues of carbonaceous material and Z-6018 silicone grafted in the ASiHBR, which are stable. In air atmosphere, the residue is only SiO_2; all other components of the ASiHBR underwent complete combustion—as seen in Figure 7. The thermal stability of our resins increases with the initial silicone content. The grafting efficiency (GE) of the silicone was

TABLE II
M_n Values for ASiHBRs

ASiHBR	Intercept ($\times 10^2$)	M_n (g/mole)
ASiHBR1	2.15	7.75×10^3
ASiHBR2	1.94	8.59×10^3
ASiHBR3	1.71	9.75×10^3
ASiHBR4	1.53	10.9×10^3

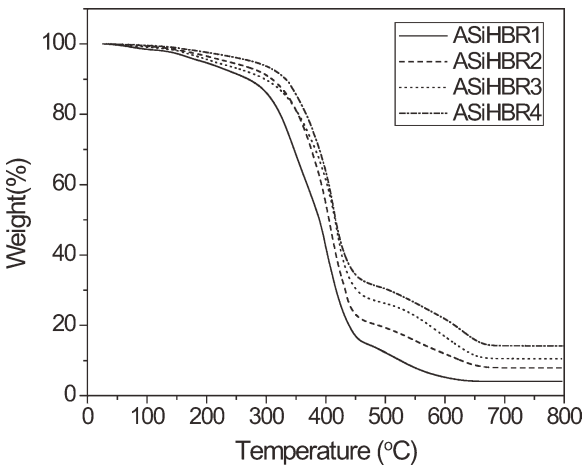

Figure 7 Acid values as a function of time.

TABLE III
Thermogravimetric Analysis Results

Resins	T_{d1} (N_2)	T_{d2} (N_2)	% Residue (SiO_2)	% Si final	Efficiency
ASiHBR1	302	–	4.09	1.91	93.6
ASiHBR2	317	501	7.92	3.69	98.4
AsiHBR3	334	494	10.52	4.91	94.6
ASiHBR4	354	506	14.11	6.58	91.0

determined from TGA results in air in terms of the initial (a) and the final (b) silicon content as:

$$GE = a/b \times 100 \quad (2)$$

The efficiency increases with the silicone content in the residue; see Table III. Silicone polymerization is a possible side reaction, because there is competition between grafting of Z-6018 in the resin and homopolymerization of the Z-6018 silicone—as reported by Kanai et al.[23] for resins with low branching degrees. We note that aromatic rings on the silicone compound are voluminous, steric effects are possible. Despite that possible side reaction, all grafting efficiencies exceed 90%. The thermal stability of all ASiHBRs is higher than that of AHBR (267°C).[30]

HYDROLYTIC STABILITY

Polyesters are susceptible to hydrolysis reactions in water.[34] A free acid is produced. The stability of material to the degradation is inversely proportional to the amount of free acid in the system. Figure 8 shows diagrams of the AVs versus time for all materials. Clearly the ASiHBRs show higher hydrolysis resistance than AHBR. The reason is that ether groups are more stable than the ester groups against acid as well as base hydrolysis.[35] Moreover, the silicone hydrophobicity limits wetting and surface contact with water-based media. Furthermore, the reduction in susceptibility to hydrolysis also may be due to the modification process; molar mass increases and the ester groups are less exposed to hydrolysis since they are further away from the peripheries.

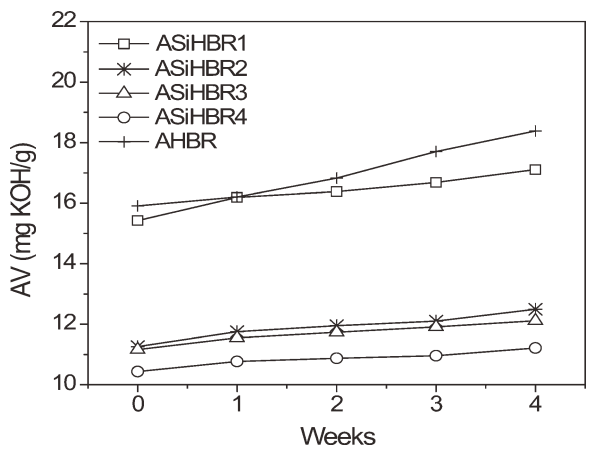

Figure 8 Bode diagrams of the resins studied.

In Table IV, we provide absolute variations of the AV (the differences between the initial and the final values) and also the respective percentage changes (the variation divided by the initial value in %).

ANTICORROSIVE BEHAVIOR OF COATINGS

Anticorrosive properties of our resins were determined by EIS.[36] The electrical resistance of a coating is a general indication of its performance as an anticorrosive material. With an electrochemical cell in the on position, impedance Z is defined as the ability of a circuit to resist or prevent the flow of electric current[37]:

$$Z = E/I \quad (3)$$

Here E is the potential and I the current. When an organic coating acts as a highly efficient barrier against water and oxygen penetration, a high value of Z is obtained.[38] The impedance of an electrochemical system can be studied as a function of the frequency of an applied alternating current (Bode diagram) or from plots of imaginary impedance Z_{im} versus real impedance Z_{re} (Nyquist diagram).[39]

The Bode diagram allow to detect small impedances in presence of large impedances while the Nyquist diagram does not have this advantage. For example, in the Nyquist diagram for two materials with impedance values of 10^{-6} and 10^{-8} Ω cm^2, respectively, the diagram for the impedance value of

TABLE IV
Variation of Acid Value and Variation Percentage of AV for Resins

Resins	Final AV	Variation on AV	Variation percentage on AV
ASiHBR1	17.11	1.69	10.96
ASiHBR2	12.49	1.23	10.92
ASiHBR3	12.11	0.95	8.51
ASiHBR4	11.21	0.78	7.48
AHBR	19.89	3.99	25.06

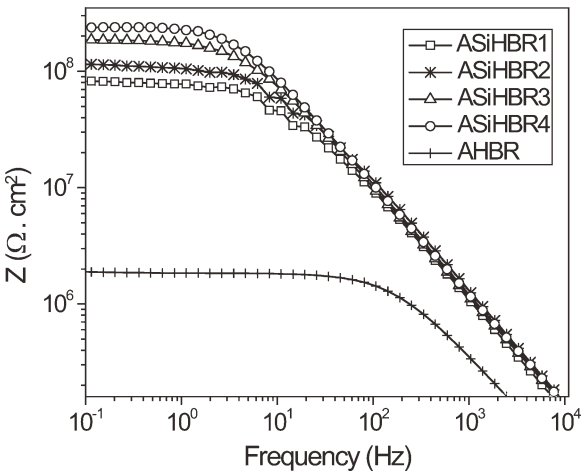

Figure 9 Impedance versus frequency diagrams of the resins studied.

10^{-6} Ω cm^2 would appear like a point only. On the other hand, the advantage of the Nyquist diagram with respect to the Bode diagram is that the former allows determination of the polarization resistance and the solution resistance. In the presence of large differences in impedance values, one can determine polarization resistance R_{po} (initial value of Z_{re}) and final resistance Z_{re} of the coating film called R_{so}[39] before reduction by passage of 3.5 wt % aqueous sodium chloride solution. In Figure 9, we provide the Bode diagram of our resins. All ASiHBRs show higher Z values than AHBR, an indication of improved corrosion resistance. The Z values at the angular frequency of 0.1 Hz angular frequency increase with the contents of silicone present: The Z values of the resins at 0.1 Hz frequency are the following: $Z = 8.21 \times 10^7$ Ω cm^2 for ASiHBR1; 1.14×10^8 Ω cm^2 for ASiHBR2; 1.85×10^8 Ω cm^2 for ASiHBR3; and 2.36×10^8 Ω cm^2 for ASiHBR4. This while the value for AHBR is 1.69×10^6 Ω cm^2.

We have taken photographs of the resin films after impedance analysis; see Figure 10. We see how extensive corrosion has taken place in the AHBR material. In Figure 11, we show the Nyquist diagrams: of the ASiHRs [Fig. 11(a)] and the AHBR [Fig. 11(b)]. Values of R_{po} and R_{so} were obtained from these diagrams. These parameters increase with the contents of silicon in a substantial way (Table V). The value of polarization resistance is inversely proportional to the corrosion rate; therefore, the ASiHBR4 material has the highest corrosion resistance. After an initial increase of Z_r, all curves in Figure 11(a) show a maximum and then a decrease. A possible reason is ionic transference from films to the NaCl solution; such behavior has been reported before.[40]

AHBR shows an increase of Z and then a loop which can be explained by deterioration of the resin film,[41] formation of corrosion products,[42–44] or else by a charge transfer between the substrate and the resin.[45,46] Initial corrosion resistance of 10^6 Ω cm^2 is considered poor[47] while values of the order of 10^8 Ω cm^2 are considered excellent. Table V shows that we

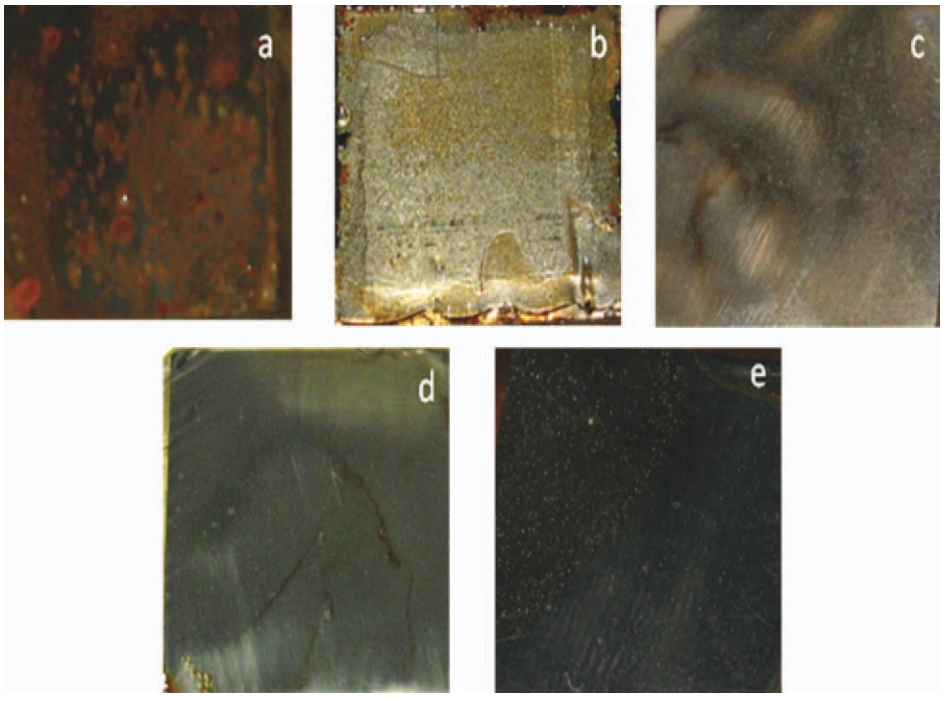

Figure 10 Photographs of the resin films after impedance analysis. [Color figure can be viewed in the online issue, which is available at wileyonlinelibrary.com.]

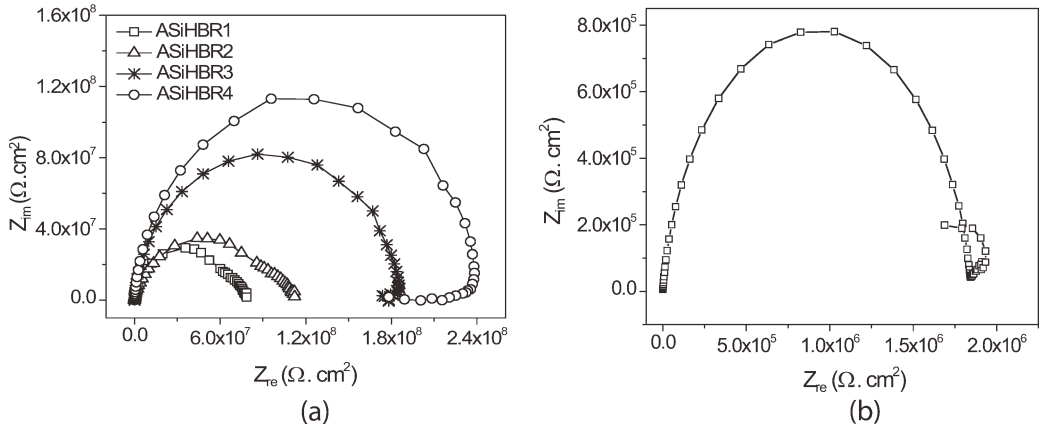

Figure 11 Nyquist diagrams.

TABLE V
R_{so} and R_{po} Values for the Resins

Resins	R_{so} (Ω.cm^2)	R_{po} (Ω.cm^2)
ASiHBR1	6.19×10^2	8.21×10^7
ASiHBR2	8.84×10^2	1.14×10^8
ASiHBR3	1.19×10^3	1.85×10^8
ASiHBR4	1.54×10^3	2.36×10^8
AHBR	5.25×10^2	1.84×10^6

have at least three coating materials in the latter category.

TRIBOLOGICAL PROPERTIES

Friction can be either static or dynamic,[48,49] we determine here the latter. We present the results in Figure 12. We see a dramatic effect of grafting of the silicone compound onto our resin. The higher the silicone content, the lower the dynamic friction. Our results agree with those reported in the literature on silicone-containing materials.[50] For that matter, the presence of silica decreases the friction.[51]

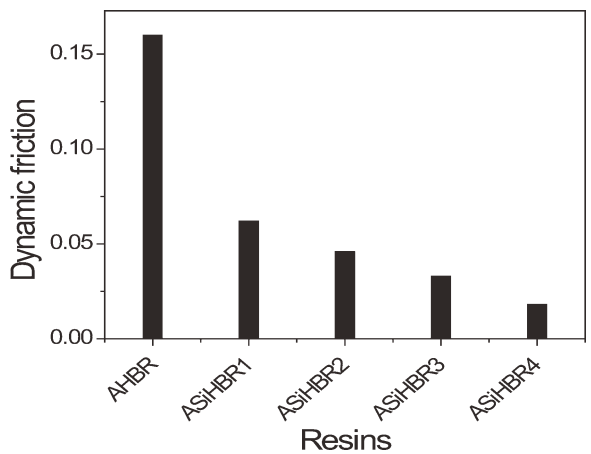

Figure 12 Dynamic friction results.

References

1. Pilch-Pitera, B. Przemysl Chem 2009, 88, 892.
2. Mohamed, H. A.; Farag, A. A.; Badran, B. M. J Appl Polym Sci 2010, 117, 1270.
3. Chandler-Temple, A.; Wentrup-Byrne, E.; Whittaker, A. K.; Grøndahl, E. J Appl Polym Sci 2010, 117, 3331.
4. Pilch-Pitera, B. J Appl Polym Sci 2010, 117, 3613.
5. Pilch-Pitera, B.; Stagraczynski, R. J Appl Polym Sci 2010, 118, 3586.
6. Slinckx, M.; Henry, N.; Krebs, A.; Uytterhoeven, G. Prog Org Coat 2000, 38, 163.
7. Zagar, E.; Zigon, M.; Podzimek, S. Polymer 2006, 47, 166.
8. Malstrom, E.; Hult, A. Macromolecules 1996, 29, 1222.
9. Murillo, E. A.; Vallejo, P. P.; Sierra, L.; López, B. L. J Appl Polym Sci 2009, 112, 200.
10. Haselmann, R.; Holter, D.; Frey, H. Macromolecules 1998, 31, 3790.
11. Kim, Y. H.; Webster, O. W. Macromolecules 1992, 25, 5561.
12. Bruchmann, B.; Koniger, R.; Renz, H. Macromol Symp 2002, 44, 271.
13. Manczyk, K.; Szewczyk, P. Prog Org Coat 2002, 44, 99.
14. Karacaya, C.; Gunduz, G.; Aras, L.; Mecidoglu, I. A. Prog Org Coat 2007, 59, 265.
15. Lindeboom, J. Prog Org Coat 1998, 34, 147.
16. Jikei, M.; Kakimoto, M. Prog Polym Sci 2001, 26, 1233.
17. Magnusson, H.; Malmstrom, E.; Hult, A.; Johansson, M. Polymer 2002, 43, 301.
18. Bat, E.; Gunduz, G. Prog Org Coat 2006, 55, 330.
19. Soucek, M. D.; Dworak, D. P.; Chakraborty, R. J. Coat Technol Res 2007, 4, 263.
20. Easton, T.; Poultney, S. J Coat Technol Res 2007, 4, 187.
21. Park, H. S.; Yang, I.; Wu, J. P.; Kim, M.; Hanm, H.; Kim, S.; Rhee, H. J Appl Polym Sci 2000, 81, 1614.
22. Bilyeu, B.; Brostow, W.; Chudej, L.; Estevez, M.; Hagg, H. E.; Rodriguez, J. R.; Vargas, S. Mater Res Innovat 2007, 11, 181.
23. Kanai, T.; Mahato, T. K.; Kumar, D. Prog Org Coat 2007, 58, 259.
24. Brostow, W., Ed. Performance of Plastics; Hanser, Munich: Cincinnati, 2000.
25. Brostow, W.; Datashvili, T.; Huang, B. Polym Eng Sci 2008, 48, 292.
26. Brostow, W.; Datashvili, T. Mater Res Innovat 2007, 11, 127.
27. Brostow, W.; Chonkaew, W.; Menard, K. P.; Scharf, T. W. Mater Sci Eng A 2009, 507, 241.
28. De la Isla, A.; Brostow, W.; Bujard, B.; Estevez, M.; Rodriguez, J. R.; Vargas, S.; Castaño, V. M. Mater Res Innovat 2003, 7, 110.
29. Ozgumus, S.; Iyim, T. B.; Acar, I.; Kucukoglu, E. Polym Adv Technol 2007, 18, 213.

30. Murillo, E. A.; Vallejo, P. P.; López, B. L. Prog Org Coat 2010, 69, 235.
31. Murillo, E. A.; Vallejo, P. P.; López, B. L. J Appl Polym Sci 2011, 120, 3151.
32. Pathak, S. S.; Sharma, A.; Khanna, A. S. Prog Org Coat 2009, 65, 288.
33. Schröder, E.; Müller, G.; Arndt, K. F. Polymer Characterization; New York: Hanser Publishers, Munich, Vienna, 1988.
34. Wang, C.; Jones, F. N. J Appl Polym Sci 2000, 78, 1698.
35. Chikh, L.; Tessier, M.; Fradet, A. Polymer 2007, 48, 1884.
36. Amirudin, A.; Thierry, D. Prog Org Coat 1995, 26, 1.
37. Delahay, P. New Instrumental Methods in Electrochemistry; Interscience: New York, 1954.
38. Skale, S.; Dolecek, V.; Slemnik, M. Prog Org Coat 2008, 62, 387.
39. Gonzalez, J. A.; Otero, E.; Bautista, A.; Almeida, E.; Morcillo, M. Prog Org Coat 1998, 33, 61.
40. Qi, X.; Vetter, C.; Harper, A. C.; Gelling, V. J Prog Org Coat 2008, 63, 345.
41. Masadeh, S. J Miner Mater Character Eng 2005, 4, 75.
42. Fedrizzi, L.; Rodriguez, F. J.; Rossi, S.; Deflorian, F; Di Maggio, R. Electrochim Acta 2001, 46, 3715.
43. Veleva, L.; Chin, J.; Del Amo, B. Prog Org Coat 1999, 36, 211.
44. Bonora, P. L.; Deflorian, F.; Fedrizzi, L. Electrochim Acta 1996, 41, 1073.
45. Gonzalez-García, Y.; Gonzalez, S.; Souto, R. M. Corrosion Sci 2007, 49, 3514.
46. Del Amo, B.; Romagnoli, R.; Deyá, C.; González, J. A. Prog Org Coat 2002, 45, 389.
47. McIntyre, J. M.; Pham, H. Q. Prog Org Coat 1996, 27, 201.
48. Brostow, W.; Deborde, J.; Jaklewicz, M.; Olszynski, P. J Mater Ed. 2003, 24, 119.
49. Brostow, W.; Kovacevic, V.; Vrsaljko, D.; Whitworth, J. J Mater Ed 2010, 32, 273.
50. Shi, G.; Zhang, M. Q.; Rong, M. Z.; Wetzel, B.; Friedrich, K. Wear 2003, 254, 784.
51. Dasari, A.; Yu, Z.-Z.; Mai, Y.-W. Mater Sci Eng R 2009, 63, 31.